Evaluation of Antiatherogenic Properties of Ezetimibe Using ^{3}H-Labeled Low-Density-Lipoprotein Cholesterol and ^{99m}Tc-cAbVCAM1–5 SPECT in ApoE^{−/−} Mice Fed the Paigen Diet

Laurent S. Dumas*[1–3], François Briand*[4], Romain Clerc[1,2,4], Emmanuel Brousseau[4], Christopher Montemagno[1,2], Mitra Ahmadi[1,2], Sandrine Bacot[1,2], Audrey Soubies[1,2], Pascale Perret[1,2], Laurent M. Riou[1,2], Nick Devoogdt[5], Tony Lahoutte[5], Gilles Barone-Rochette[1,2,6], Daniel Fagret[1,2,6], Catherine Ghezzi[1,2], Thierry Sulpice[4], and Alexis Broisat[1,2]

[1]INSERM U1039 Radiopharmaceutiques Biocliniques, Grenoble, France; [2]UGA, Université Grenoble Alpes, Grenoble, France; [3]Advanced Accelerator Applications, Saint-Genis-Pouilly, France; [4]Physiogenex, Labège, France; [5]ICMI, Vrije Universiteit Brussel, Brussels, Belgium; and [6]CHRU Grenoble, Hôpital Michallon, Grenoble, France

The addition of ezetimibe, an intestinal cholesterol absorption inhibitor, to statin therapy has recently shown clinical benefits in the Improved Reduction of Outcomes: Vytorin Efficacy International Trial by reducing low-density-lipoprotein (LDL) cholesterol levels more than statin therapy alone. Here, we investigated the mechanisms by which inhibition of intestinal cholesterol absorption might contribute to the clinically observed reduction in cardiovascular events by evaluating its effect on inflammatory plaque development in apolipoprotein E[−/−] mice. **Methods:** Apolipoprotein E[−/−] mice were fed the Paigen diet (1.25% cholesterol, 0.5% cholic acid, and 15% fat) without or with ezetimibe (7 mg/kg/d) for 6 wk. In a first set of mice (n = 15), we intravenously injected ^{3}H-cholesteryl oleate–labeled human LDL to test whether ezetimibe promotes LDL-derived cholesterol fecal excretion. In a second set (n = 20), we used the imaging agent ^{99m}Tc-cAbVCAM1–5 to evaluate expression of an inflammatory marker, vascular cell adhesion molecule 1 (VCAM-1), in atherosclerotic plaques. In a third set (n = 21), we compared VCAM-1 expression with ^{99m}Tc-cAbVCAM1–5 uptake in various tissues. **Results:** Mice treated with ezetimibe showed a 173% higher LDL–cholesteryl ester plasma disappearance rate (P < 0.001 vs. control) after ^{3}H-cholesteryl oleate–labeled LDL injection. At 96 h after injection, the hepatic fraction of ^{3}H-tracer was 61% lower in mice treated with ezetimibe (P < 0.001). Meanwhile, LDL-derived ^{3}H-cholesterol excretion in the feces was 107% higher (P < 0.001). The antiatherogenic effect of ezetimibe monitored by ^{99m}Tc-cAbVCAM1–5 SPECT showed a 49% reduction in aortic tracer uptake (percentage injected dose per cubic centimeter, 0.95 ± 0.04 vs. 1.87 ± 0.11; P < 0.01). In addition to hypercholesterolemia, the proinflammatory Paigen diet significantly increased VCAM-1 expression with respect to the control group in various tissues, including the aorta, and this expression correlated strongly with ^{99m}Tc-cAbVCAM1–5 uptake (r = 0.75; P < 0.05). **Conclusion:** Inhibition of intestinal cholesterol absorption with ezetimibe promotes antiatherosclerotic effects through increased LDL cholesterol catabolism and LDL-derived cholesterol fecal excretion and reduces inflamed atherosclerotic plaques. These mechanisms may contribute to the benefits of adding ezetimibe to a statin therapy.

Key Words: atherosclerosis; ezetimibe; LDL-cholesterol catabolism; VCAM-1; ^{99m}Tc-cAbVCAM1–5

Cardiovascular diseases are caused mainly by coronary artery disease and, more specifically, by rupture of a vulnerable atherosclerotic plaque (1). To prevent cardiovascular events, lowering low-density-lipoprotein (LDL) cholesterol levels with statins is the most widely used therapy (2). Nevertheless, some patients treated with statins are not reaching low-enough levels of LDL cholesterol or experience adverse effects (3), calling for alternative LDL-lowering therapies.

Ezetimibe is a dietary and biliary intestinal cholesterol absorption inhibitor that selectively inhibits the Niemann-Pick C1-like 1 receptor without affecting intestinal absorption of triglycerides (4). Davis et al. demonstrated that ezetimibe decreased plasma cholesterol levels by 61% and reduced the development of atherosclerotic lesions in apolipoprotein E[−/−] (ApoE^{−/−}) mice (5). Ezetimibe is prescribed as a second-line therapy (6), and its effectiveness for reducing LDL cholesterol levels has been demonstrated in several clinical studies (7,8). Moreover, a beneficial 22% reduction in LDL cholesterol levels has been reported when ezetimibe was given together with a statin, as compared with a statin alone (9). Results from a clinical trial, Improved Reduction of Outcomes: Vytorin Efficacy International Trial, that started in 2005 showed that reducing LDL cholesterol levels below the recommended target by adding ezetimibe to simvastatin treatment granted an additional benefit by significantly reducing cardiovascular events, as compared with treatment using simvastatin alone, in subjects with acute coronary syndrome (10). Interestingly, ezetimibe in combination with a statin significantly decreased the levels of C-reactive protein and might have metabolic effects other than simply the lowering of LDL cholesterol levels (11,12).

In the present study, we aimed to investigate the mechanisms by which ezetimibe might reduce cardiovascular events. We investigated whether blocking intestinal cholesterol absorption may promote fecal excretion of atherogenic cholesterol deriving from LDL particles. The effect of ezetimibe on LDL cholesterol metabolism and LDL-derived cholesterol fecal excretion was therefore evaluated with ^{3}H-cholesteryl oleate–labeled LDL kinetics, and its effect on inflammatory plaque development was evaluated using ^{99m}Tc-cAbVCAM1–5 imaging in ApoE$^{-/-}$ mice fed the Paigen diet. ^{99m}Tc-cAbVCAM1–5, currently under clinical translation, is a SPECT radiotracer directed against the inflammatory marker vascular cell adhesion molecule 1 (VCAM-1) (13,14). This molecular imaging agent belongs to a new class of radiotracer derived from single-domain antibodies, or variable domain of the heavy chain of the heavy-chain antibody, which are composed of the single variable domain of camelidae immunoglobulins. Aortic atherosclerotic lesions have been successfully detected in ApoE$^{-/-}$ mice fed a western diet using ^{99m}Tc-cAbVCAM1–5 imaging, and the sensitivity of this tool has been demonstrated using statin therapy as a gold standard (13,14). This molecular imaging agent can therefore be used for the preclinical noninvasive evaluation of antiatherosclerotic therapies.

MATERIALS AND METHODS

Animals and Diet

All experimental procedures were in accordance with institutional guidelines and approved by the animal care and use committees of Midi-Pyrénées and Grenoble University. Seven-week-old female mice were used. Fifty ApoE$^{-/-}$ mice were fed a proatherogenic Paigen diet (1.25% cholesterol, 0.5% cholic acid, and 15% fat) supplemented (Paigen+eze), or not (Paigen), with ezetimibe (0.005% in diet, equivalent to 7 mg/kg/d) for 6 wk. Six C57BL6/J mice were fed a chow diet to serve as a control. Body weight and food consumption were monitored weekly.

The effect of ezetimibe on LDL cholesterol metabolism and LDL-derived cholesterol fecal excretion in vivo was evaluated using ^{3}H-cholesteryl oleate–labeled LDL kinetics ($n = 15$), and the effect of ezetimibe on atherosclerosis development and inflammation was investigated through in vivo SPECT and postmortem analysis ($n = 41$).

Effect on LDL Cholesterol Metabolism and Fecal Excretion

LDL particles were isolated from human plasma by ultracentrifugation ($1.019 <$ density < 1.063), extensively dialyzed, and then labeled with ^{3}H-cholesteryl oleate in the presence of lipoprotein-deficient serum isolated from human plasma, as described previously (15). After isolation of labeled LDL by ultracentrifugation and extensive dialysis, the mice (7 in the Paigen group and 8 in the Paigen+eze group) were weighed, individually caged for feces collection, and injected intravenously with ^{3}H-cholesteryl oleate–labeled LDL (~3–4 million disintegrations/min/mouse).

Blood was collected from the tail tip at 5 min and then 1, 3, 6, 24, and 48 h after intravenous injection to isolate plasma (5 μL) and count ^{3}H-radioactivity. The plasma ^{3}H-tracer decay curve was then used to calculate the LDL–cholesteryl ester fractional catabolic rate (i.e., the fraction of tracer irreversibly removed from the plasma per unit of time) using the SAAM II software program (The Epsilon Group), as described previously (16).

The mice were kept in individual cages for up to 96 h after tracer injection to collect feces and to measure fecal ^{3}H-cholesterol and ^{3}H-bile acids after chemical extraction, as described previously (15). The mice were then euthanized and exsanguinated. The liver was harvested and weighed. An approximately 50-mg liver sample was used to measure ^{3}H-radioactivity in the whole liver as well as in the cholesterol

and bile acid fractions. Hepatic and fecal total cholesterol and bile acid masses were also measured from the same samples using colorimetric kits, as described previously (17), and tracer recovery was expressed as percentage injected dose (%ID).

Effect on Atherosclerosis Development and Inflammation

In Vivo SPECT. In vivo SPECT of inflamed atherosclerotic lesions was performed using ^{99m}Tc-cAbVCAM1–5 in 10 Paigen mice and 10 Paigen+eze mice. cAbVCAM1–5 was radiolabeled as previously described using the tricarbonyl method (13). A SPECT/CT acquisition was performed 2 h after the intravenous injection of 47.2 ± 10.7 MBq of ^{99m}Tc-cAbVCAM1–5, and aortic uptake was expressed as %ID/cm^3 (13).

Postmortem Analysis. Frozen sections of aortic root were obtained for histologic examination, VCAM-1 immunostaining, and ^{99m}Tc-cAbVCAM1–5 autoradiography. Plaque surface area was expressed as square millimeters. VCAM-1 intensity was graded as low (1), moderate (2), or strong (3) by 2 masked observers. ^{99m}Tc cAbVCAM1–5 uptake in autoradiographic images was expressed either as a concentration (%ID/g) or as the total uptake per slice (%ID/slice), as previously described (14).

VCAM-1 protein expression was further investigated by ELISA in 9 Paigen mice, 6 Paigen+eze mice, and 6 control mice. Three hours after injection of ^{99m}Tc-cAbVCAM1–5, the mice were euthanized by CO$_2$ inhalation. Tissues of interest were rapidly harvested, rinsed in 0.9% NaCl, and weighed. ^{99m}Tc-cAbVCAM1–5 uptake was measured by γ-well counting (Wizard^2; PerkinElmer). After the tissue had been processed with a Potter–Elvehjem tissue grinder in ice-cold radioimmuno-precipitation assay buffer, the homogenates were centrifuged at $10,000g$ for 10 min at 4°C. The supernatants were extracted and the VCAM-1 protein level was quantified using a commercial kit (sVCAM-1/CD-106; R&D Systems).

Western blot analysis was used to evaluate whether ezetimibe has a direct antiinflammatory effect on VCAM-1 expression in human THP1 monocytes. The human THP1 cell line was cultured in RPMI 1640 (Sigma-Aldrich) containing 10% heat-inactivated fetal bovine serum, supplemented with 2 mM glutamine and 1% penicillin/streptomycin at 37°C in an atmosphere of 5% CO$_2$. A total of 1×10^6 cells per well were suspended in 6-well plates and differentiated into macrophages for 24 h with phorbol 12-miristate 13-acetate at 5 ng/mL in the presence or absence of ezetimibe (100 nM). Then, the cells were rinsed with RPMI 1640 and allowed to rest for 24 h. Differentiated THP1 macrophages were stimulated with TNF-α at 50 ng/mL for 24 h with or without ezetimibe treatment (100 nM). After treatment, the cells were rinsed with phosphate-buffered saline and lysed with ice-cold radioimmunoprecipitation assay buffer at −80°C. Cell lysates were centrifuged at $10,000g$ for 10 min at 4°C, and the supernatant was collected. Protein was quantified by the bicinchoninic acid method, and 30-μg protein samples were loaded into sodium dodecyl sulfate–polyacrylamide gel (7.5%) and then transferred on a nitrocellulose membrane. Rabbit anti–VCAM-1 antibody (ab13047; Abcam) was used as the primary antibody at 1/1,000 at 4°C overnight. Goat antirabbit (horseshoe peroxidase–labeled goat antirabbit IgG; Dako) was used as the secondary antibody at 1/2,000 at room temperature for 1 h. The protein signal, observed at 110 kDa, was quantified using ImageJ software and normalized to the expression of α-actin.

Statistical Analysis

All results are presented as mean $\pm$ SEM. Student *t* testing was used to compare datasets of equal variance, and Mann–Whitney U testing was used for unpaired datasets of unequal variance. The significance of linear correlations was assessed with Pearson testing. Multiple-comparison statistical testing was used to compare data
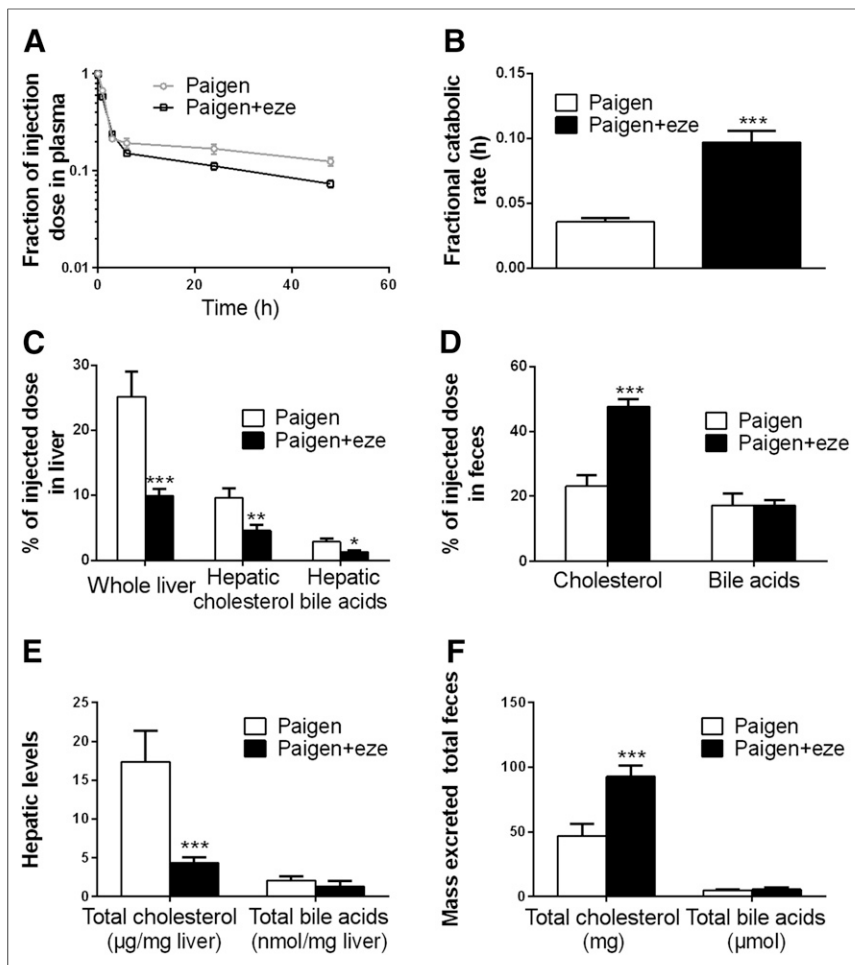
FIGURE 1. Effect of ezetimibe on LDL cholesterol metabolism and excretion using in vivo ^{3}H-cholesteryl: ^{3}H-tracer plasma disappearance (A), LDL–cholesteryl ester fractional catabolic rate (B), hepatic (C) and fecal (D) ^{3}H-tracer tracer recovery after ^{3}H-cholesteryl oleate–labeled human LDL intravenous injection, and hepatic (E) and fecal (F) total cholesterol and bile acid mass in ApoE$^{-/-}$ mice. *$P < 0.05$ vs. Paigen group. **$P < 0.01$ vs. Paigen group. ***$P < 0.001$ vs. Paigen group.

among the 3 groups (Paigen, Paigen+eze, and control). The significance level was set at a P value of less than 0.05.

RESULTS

Effect on Plasma Cholesterol Levels and Body Weight

Treatment with ezetimibe significantly reduced total cholesterol levels in plasma (Paigen, 29.0 ± 3.1 mmol/L, and Paigen+eze, 14.6 ± 2.3 mmol/L; $P < 0.01$). Moreover, body weight was significantly higher in the ezetimibe-treated group than in the control group (21.0 ± 0.2 g vs. 18.4 ± 0.5 g, $P < 0.01$) (Supplemental Table 1; supplemental materials are available at http://jnm.snmjournals.org).

Effect on LDL Cholesterol Metabolism and Fecal Excretion

After injection of ^{3}H-cholesteryl oleate–labeled human LDL, mice that were treated with ezetimibe showed a higher rate of ^{3}H-tracer disappearance than mice that were not (Fig. 1A), resulting in a 173% higher ($P < 0.001$) LDL–cholesteryl ester catabolism (Fig. 1B). At 96 h after radiolabeled LDL injection, ^{3}H-tracer recovery in the whole liver was reduced by 61% with ezetimibe ($P < 0.001$), and accordingly, the fractions of ^{3}H-tracer recovery in he-

patic cholesterol and hepatic bile acids were also significantly reduced, by 55% and 52%, respectively (Fig. 1C). Meanwhile, the fraction of ^{3}H-tracer recovery in fecal cholesterol was increased by 107% ($P < 0.001$) (Fig. 1D). Similar trends were observed for hepatic cholesterol level (Fig. 1E) and fecal cholesterol mass excretion (Fig. 1F), with ezetimibe resulting in a 75% reduction and 99% increase, respectively (both $P < 0.001$).

Effect on Atherosclerosis Development and Inflammation

In Vivo SPECT. VCAM-1 expression was successfully evaluated noninvasively using in vivo ^{99m}Tc-cAbVCAM1–5 SPECT/CT to investigate the effect of ezetimibe on atherosclerosis-related inflammation. ^{99m}Tc-cAbVCAM1–5 uptake in the ascending aorta was visible in the Paigen group and was decreased by 49% when the Paigen diet was supplemented with ezetimibe (1.87 ± 0.11 %ID/cm^3 vs. 0.95 ± 0.04 %ID/cm^3, $P < 0.001$) (Fig. 2D; Supplemental Fig. 1).

Postmortem Analysis. The Paigen diet induced rapid atherosclerotic plaque formation in the aortic root of ApoE$^{-/-}$ mice (0.33 ± 0.03 mm^2), which was significantly reduced by 73% by ezetimibe (0.11 ± 0.03 mm^2, $P < 0.0001$). Histologically, as demonstrated by hematoxylin erythrosine saffron quantification, this was attributed to a significant decrease in core thickness and, therefore, intima-to-media ratio, whereas cap thickness remained unchanged (Fig. 2A and Supplemental Fig. 2). Moreover, as determined by VCAM-1 immunostaining, VCAM-1 score in atherosclerotic lesions was significantly reduced in ezetimibe-treated mice (1.56 ± 0.23 vs. 2.4 ± 0.18, $P < 0.01$) (Fig. 2B). Accordingly, on ex vivo ^{99m}Tc-cAbVCAM1–5 autoradiography, aortic uptake was significantly reduced in ezetimibe-treated mice (Fig. 2C). Indeed, ^{99m}Tc-cAbVCAM1–5 density was 39% lower in the ezetimibe-treated group than in the untreated group (2.7 ± 0.29 %ID/g vs. 4.4 ± 0.38 %ID/g, $P < 0.01$). Overall, the ezetimibe-induced decreases in VCAM-1 expression and burden of atherosclerotic lesions resulted in a profound, 81%, reduction in total ^{99m}Tc-cAbVCAM1–5 aortic uptake.

VCAM-1 protein expression was further investigated in various tissues by ELISA (Fig. 3). Low levels of VCAM-1 were found in the aortas of control mice, and no difference in the VCAM-1 expression of lesion-free abdominal aortas was found among the experimental groups. The Paigen diet induced a significant, 11-fold, increase in the ascending aorta and aortic arch of ApoE$^{-/-}$ mice. This effect was significantly inhibited by ezetimibe (Fig. 3A). Indeed, VCAM-1 expression in the ascending aorta was reduced by 47% in the ezetimibe-treated Paigen group in comparison to the untreated Paigen group (2.40 ± 0.60 ng/mg vs. 4.54 ± 0.37 ng/mg, $P < 0.05$) (Fig. 3A). ^{99m}Tc-cAbVCAM1–5 aortic uptake correlated with this VCAM-1 expression pattern. Indeed,
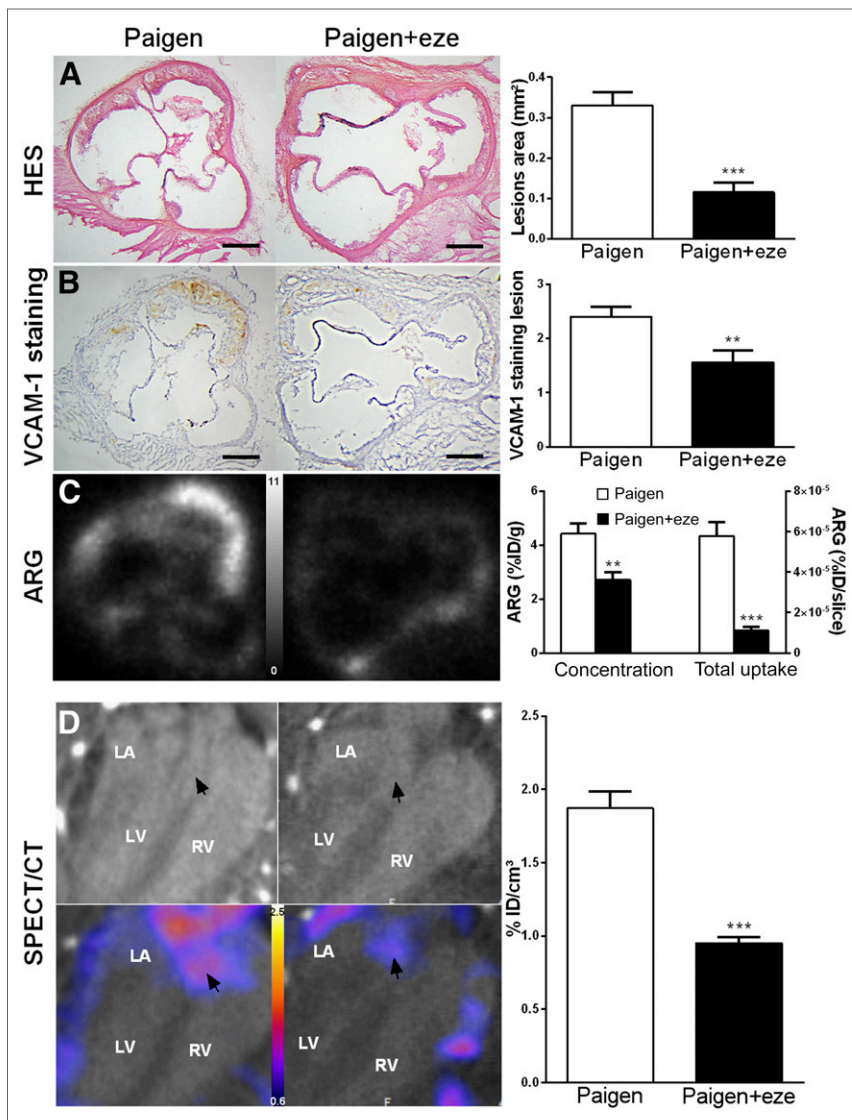
FIGURE 2. Effect of ezetimibe on plaque inflammation. (A and B) Paigen diet–induced aortic lesions and ezetimibe significantly reduced plaque volume and VCAM-1 expression as determined by histology (A) and immunohistochemistry (B). (C) As shown on autoradiographic images, ^{99m}Tc-cAbVCAM1–5 aortic uptake was significantly reduced in ezetimibe-treated mice when expressed either as concentration or as total uptake per slice. (D) In vivo quantification of ^{99m}Tc-cAbVCAM1–5 aortic uptake was in accordance with ex vivo data, and effect of ezetimibe was successfully monitored as shown on representative CT and SPECT/CT coronal views selected at level of aortic roots (arrows). **$P < 0.01$ vs. Paigen. ***$P < 0.001$ vs. Paigen. Scale bar = 200 μm; autoradiography scale = 0–11 %ID/g; SPECT scale = 0.8–2.6 %ID/cm³. ARG = autoradiography; HES = hematoxylin erythrosine saffron; LA = left atrium; LV = left ventricle; RV = right ventricle

^{99m}Tc-cAbVCAM1–5 uptake in atherosclerotic lesions increased significantly in the untreated Paigen group, and ezetimibe treatment significantly reduced this effect by approximately 50% (3.97 ± 0.31 %ID/g vs. 1.98 ± 0.5 %ID/g, $P < 0.01$) (Fig. 3B). Consequently, ^{99m}Tc-cAbVCAM1–5 uptake strongly correlated with VCAM-1 expression in the aorta ($R = 0.76$, $P < 0.0001$) (Supplemental Fig. 3). Interestingly, the Paigen diet also induced an increase in VCAM-1 expression in all other investigated tissues, which reached statistical significance in the liver, spleen, thymus, and heart. This effect was significantly reduced by ezetimibe in the liver, thymus, heart, and muscle (Fig. 4A). As observed in the

aorta, the biodistribution profile of ^{99m}Tc cAbVCAM1–5 correlated with that of VCAM-1 expression. Indeed, the Paigen diet induced an increase in ^{99m}Tc-cAbVCAM1–5 uptake in all investigated tissues, reaching statistical significance in the liver, spleen, and lymph nodes. This effect was significantly inhibited by ezetimibe in the thymus, heart, and muscle (Fig. 4B).

As determined in vitro on human THP1 cells by Western blot analysis, VCAM-1 expression was observed on differentiated and stimulated macrophages but not on monocytes. Interestingly, ezetimibe reduced VCAM-1 expression by 18% (Supplemental Fig. 4).

DISCUSSION

Ezetimibe is a potent lipid-lowering drug that targets the Niemann-Pick C1-like 1 receptor in enterocytes, which in turn results in inhibition of cholesterol absorption by the intestine. Consequently, ezetimibe inhibits not only absorption of exogenous dietary cholesterol but also reabsorption of biliary cholesterol. Therefore, whereas statins act on endogenous cholesterol synthesis, ezetimibe lowers circulating cholesterol by inhibiting exogenous cholesterol absorption and endogenous cholesterol reabsorption.

To our knowledge, the present study was the first to evaluate the effect of ezetimibe in vivo on ApoE$^{-/-}$ mice fed the Paigen diet, a hyperlipidemic diet containing a combination of cholesterol and cholic acid. Cholic acid is one of the two major bile acids that potentiate cholesterol influx (*18*). Therefore, ApoE$^{-/-}$ mice fed the Paigen diet exhibit pronounced hypercholesterolemia resulting in the rapid development of atherosclerotic lesions within only 6 wk. Our finding of a significant increase in LDL cholesterol catabolism and LDL-derived cholesterol fecal excretion in ezetimibe-treated mice demonstrated that use of ezetimibe to inhibit cholesterol absorption by the intestine promotes elimination of proatherogenic LDL cholesterol, thereby potentially preventing it from forming atherosclerotic plaques. The benefits of the 50% reduction in Paigen diet–induced hypercholesterolemia were quantified in vivo using SPECT performed with ^{99m}Tc-cAbVCAM1–5. This radiolabeled single-domain antibody, which is currently undergoing clinical translation, targets the inflammatory marker VCAM-1 and has been validated as a sensitive and reproducible tool for imaging inflammation in mouse atherosclerotic lesions (*14*). In the present study, atherosclerotic lesions were readily observable in the aortic root and ascending aorta on SPECT images. As demonstrated by quantification based on contrast-enhanced CT images, ezetimibe induced a 2-fold reduction in ^{99m}Tc-cAbVCAM1–5 uptake. Such a result is in accordance with the profound
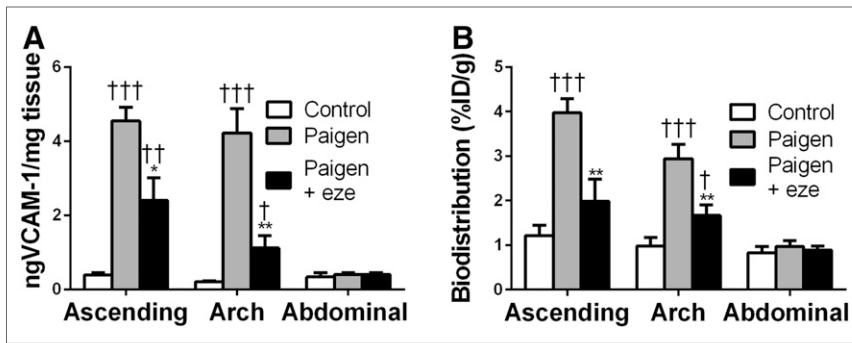
FIGURE 3. Antiinflammatory effect of ezetimibe on aortic atherosclerotic lesion. ^{99m}Tc-cAbV-CAM1–5 uptake was reduced in Paigen+eze group and correlated well with VCAM-1 expression in aorta. (A) VCAM-1 expression was evaluated on ascending aorta, aortic arch, and abdominal aorta by ELISA and expressed as nanograms of VCAM-1 per milligram of tissue. (B) ^{99m}Tc-cAbVCAM1–5 uptake was determined by γ-well counting and expressed as %ID/g. Significant P levels: **<0.01 vs. Paigen, †<0.05 vs. control, ††<0.01 vs. control, and †††<0.001 vs. control.

macrophages in the present study and may partly explain the reduction in VCAM-1 expression in the aortic sinus and aortic arch of ApoE$^{-/-}$ mice. Furthermore, the fact that ezetimibe acts on monocytes and macrophages may partly explain the reduction in VCAM-1 expression in lymphoid organs such as the spleen.

The ELISA results of the present study confirmed the 2- to 3-fold decrease in VCAM-1 protein density induced by ezetimibe in lesions in the ascending aorta and aortic arch. Moreover, the significant correlation found between the amount of VCAM-1 expressed by atherosclerotic lesions and the degree of ^{99m}Tc-cAbVCAM1–5 uptake as quantified ex vivo by γ-well counting confirmed the sensitivity of this imaging agent. Another interesting finding in our study was the significant increase in VCAM-1 expression induced by the Paigen diet in most other investigated organs—an effect that reached statistical significance in the liver, spleen, thymus, and heart and was inhibited by ezetimibe in most of them. This result is in accordance with previous studies demonstrating that the Paigen diet has not only a proatherosclerotic effect but a proinflammatory effect as well. Indeed, Vergnes et al. found that the Paigen diet induced hepatic inflammation and that this effect was attributable to the combination of cholesterol and cholic acid since removal of one of these two compounds significantly changed the pattern of proinflammatory gene expression (*21*). Our study further demonstrated that the Paigen diet induced inflammation in other organs and tissues, including the aorta, as shown by the level of VCAM-1 expression and that this effect was significantly reduced by ezetimibe. Moreover, the pattern of ^{99m}Tc-cAbVCAM1–5 biodistribution was in accordance with VCAM-1 expression in all investigated organs, suggesting that this imaging agent might be a suitable tool for noninvasive imaging of chronic inflammation in other relevant pathophysiologic settings.

Our study had some limitations. Endothelial cells and intraplaque cells expressing VCAM-1 contribute to ^{99m}Tc-cAbVCAM1–5 uptake within the lesion, and this relative contribution still needs to be determined. Image quantification and thereby inflammatory score depend on targeted cells, and an imaging agent targeting both endothelial and intraplaque cells will not provide the same information as one targeting just endothelial cells, such as anti-VCAM-1 microbubbles. Moreover, identifying the targeted cells would help us better understand the effect of a therapy on a specific cell type.

and significant 73% decrease in plaque area observed on histologic sections of the aortic root. Meanwhile, it was previously reported that ^{99m}Tc-cAbVCAM1–5 SPECT quantification in mouse atherosclerotic lesions reflects not only plaque volume but also level of VCAM-1 expression within the lesion (*14*). An interesting finding of the present study was the reduced ^{99m}Tc-cAbVCAM1–5 uptake in the atherosclerotic lesions of ezetimibe-treated mice when tracer uptake was corrected for plaque volume as demonstrated by ex vivo autoradiography. This result suggests that, independently of the reduction in plaque size, ezetimibe induced a decrease in VCAM-1 expression as well. The reduction in VCAM-1 expression might be attributed either to a decrease in cholesterolemia and the associated lipotoxicity or to a direct antiinflammatory effect of the ezetimibe as suggested by recent studies. Indeed, Muñoz-Pacheco et al. showed that ezetimibe decreased the expression of adhesion molecules (ICAM-1, CD11a, and CD11b) on THP1 monocytes and thus inhibited their differentiation into macrophagelike cells and modified the expression of micro-RNA-155, which is involved in the development of atherosclerosis (*19*). Moreover, Cerda et al. demonstrated that ezetimibe reduced the expression of micro-RNA-221, a proatherogenic micro-RNA, on tumor necrosis factor α–stimulated endothelial cells of the human umbilical vein (*20*). These results are in accordance with those obtained by Western blot analysis of THP1

FIGURE 4. Effect of ezetimibe on VCAM-1 expression in liver, spleen, thymus, heart, muscle, and lymph node. (A) VCAM-1 expression was evaluated by ELISA and expressed as nanograms of VCAM-1 per milligram of tissue. (B) ^{99m}Tc-cAbVCAM1–5 uptake was determined by γ-well counting and expressed as %ID/g. Significant P levels: *<0.05 vs. Paigen, **<0.01 vs. Paigen, †<0.05 vs. control, ††<0.01 vs. control, and †††<0.001 vs. control. LN = lymph node.

CONCLUSION

We demonstrated the antiatherogenic effect of ezetimibe on atherosclerotic plaque progression in an in vivo experimental model of ApoE$^{-/-}$ mice fed the Paigen diet. Contributing to this effect was increased LDL cholesterol catabolism and
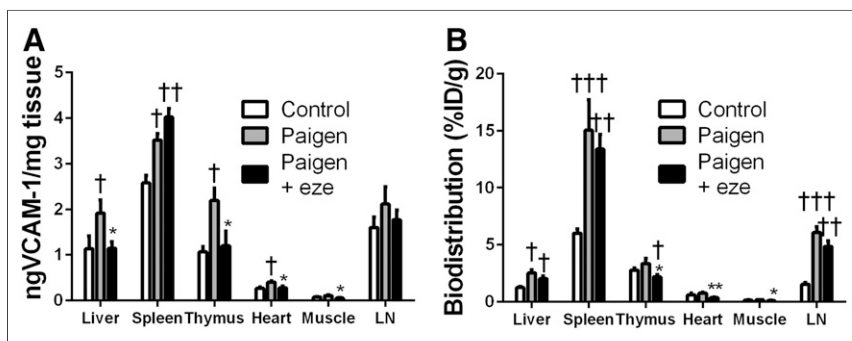
LDL-derived cholesterol fecal excretion, as well as reduced inflammation in atherosclerotic plaques as demonstrated using ^{99m}Tc-cAbVCAM1–5 imaging.

REFERENCES

1. Virmani R, Kolodgie FD, Burke AP, Farb A, Schwartz SM. Lessons from sudden coronary death: a comprehensive morphological classification scheme for atherosclerotic lesions. *Arterioscler Thromb Vasc Biol.* 2000;20:1262–1275.
2. Taylor F, Huffman MD, Macedo AF, et al. Statins for the primary prevention of cardiovascular disease. *Cochrane Database Syst Rev.* 2013;1:CD004816.
3. Armitage J. The safety of statins in clinical practice. *Lancet.* 2007;370:1781–1790.
4. Van Heek M, France CF, Compton DS, et al. In vivo metabolism-based discovery of a potent cholesterol absorption inhibitor, SCH58235, in the rat and rhesus monkey through the identification of the active metabolites of SCH48461. *J Pharmacol Exp Ther.* 1997;283:157–163.
5. Davis HR, Compton DS, Hoos L, Tetzloff G. Ezetimibe, a potent cholesterol absorption inhibitor, inhibits the development of atherosclerosis in ApoE knock-out mice. *Arterioscler Thromb Vasc Biol.* 2001;21:2032–2038.
6. Kondo Y, Hamai J, Nezu U, et al. Second-line treatments for dyslipidemia in patients at risk of cardiovascular disease. *Endocr J.* 2014;61:343–351.
7. Dujovne CA, Bays H, Davidson MH, et al. Reduction of LDL cholesterol in patients with primary hypercholesterolemia by SCH 48461: results of a multicenter dose-ranging study. *J Clin Pharmacol.* 2001;41:70–78.
8. Dujovne CA, Suresh R, McCrary Sisk C, et al. Safety and efficacy of ezetimibe monotherapy in 1624 primary hypercholesterolaemic patients for up to 2 years. *Int J Clin Pract.* 2008;62:1332–1336.
9. Ballantyne CM, Houri J, Notarbartolo A, et al. Effect of ezetimibe coadministered with atorvastatin in 628 patients with primary hypercholesterolemia: a prospective, randomized, double-blind trial. *Circulation.* 2003;107:2409–2415.
10. Cannon CP, Blazing MA, Giugliano RP, et al. Ezetimibe added to statin therapy after acute coronary syndromes. *N Engl J Med.* 2015;372:2387–2397.
11. Sager PT, Capece R, Lipka L, et al. Effects of ezetimibe coadministered with simvastatin on C-reactive protein in a large cohort of hypercholesterolemic patients. *Atherosclerosis.* 2005;179:361–367.
12. Kastelein JJP, Akdim F, Stroes ESG, et al. Simvastatin with or without ezetimibe in familial hypercholesterolemia. *N Engl J Med.* 2008;358:1431–1443.
13. Broisat A, Hernot S, Toczek J, et al. Nanobodies targeting mouse/human VCAM1 for the nuclear imaging of atherosclerotic lesions. *Circ Res.* 2012; 110:927–937.
14. Broisat A, Toczek J, Dumas LS, et al. ^{99m}Tc-cAbVCAM1–5 imaging is a sensitive and reproducible tool for the detection of inflamed atherosclerotic lesions in mice. *J Nucl Med.* 2014;55:1678–1684.
15. Briand F, Tréguier M, André A, et al. Liver X receptor activation promotes macrophage-to-feces reverse cholesterol transport in a dyslipidemic hamster model. *J Lipid Res.* 2010;51:763–770.
16. Briand F, Thieblemont Q, Muzotte E, Sulpice T. Upregulating reverse cholesterol transport with cholesteryl ester transfer protein inhibition requires combination with the LDL-lowering drug berberine in dyslipidemic hamsters. *Arterioscler Thromb Vasc Biol.* 2013;33:13–23.
17. Briand F, Tréguier M, André A, et al. Liver X receptor activation promotes macrophage-to-feces reverse cholesterol transport in a dyslipidemic hamster model. *J Lipid Res.* 2010;51:763–770.
18. Nishina PM, Verstuyft J, Paigen B. Synthetic low and high fat diets for the study of atherosclerosis in the mouse. *J Lipid Res.* 1990;31:859–869.
19. Muñoz-Pacheco P, Ortega-Hernández A, Miana M, et al. Ezetimibe inhibits PMA-induced monocyte/macrophage differentiation by altering microRNA expression: a novel anti-atherosclerotic mechanism. *Pharmacol Res.* 2012;66:536–543.
20. Cerda A, Fajardo CM, Basso RG, Hirata MH, Hirata RDC. Role of microRNAs 221/222 on statin induced nitric oxide release in human endothelial cells. *Arq Bras Cardiol.* 2015;104:195–201.
21. Vergnes L, Phan J, Strauss M, Tafuri S, Reue K. Cholesterol and cholate components of an atherogenic diet induce distinct stages of hepatic inflammatory gene expression. *J Biol Chem.* 2003;278:42774–42784.